Electronic Supplementary Material (ESI) for Soft Matter

Polymers with hydro-responsive topography identified using high throughput AFM of an acrylate microarray – Electronic supplementary information

Andrew L. Hook, Jing Yang, Xinyong Chen, Clive J. Roberts, Ying Mei, Daniel G. Anderson, Robert Langer, Morgan R. Alexander, Martyn C. Davies

ESI1. Monomers used for polymer microarray formation

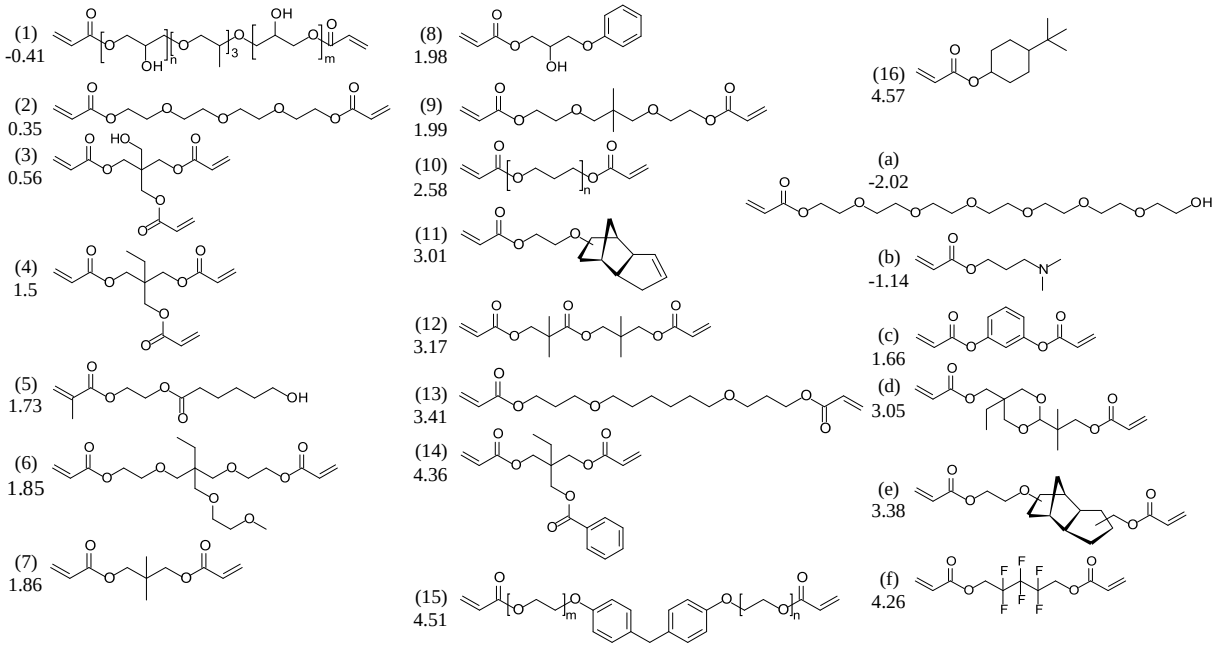

Fig. ESI1. Chemical structures of monomers. Major monomers are numbered 1-16 whilst the minor monomers are lettered a-f. The monomers are ordered from lowest to highest calculated partition constant (c*log*P) value, which is listed for each monomer under its assigned number/letter.

ESI2. Setup and optimisation of high throughput AFM imaging

Atomic force microscoy (AFM) measurements were taken using a D3000A AFM (Veeco, Santa Barbara, CA, USA) equipped with a motorised x-y-stage. Initially, the sample was placed on the stage and held in place with magnets. The microscope was then driven to the centre of the three polymer spot situated in the corners of the 24x24 array and the coordinates were used to calculate the positions of all 576 spots using a self-developed macro in Microsoft Excel, which also allowed adjustments to the number of rows and columns of the array and the number and geometrical separation between repeat measurements on each spot. This approach accounts for discrepancies between the alignment of the AFM's x-y-stage and the array. The predicted positions were inputted into a position list compatible with the 'programmed move' option of the NanoScope 5.31R1 software. The microscope was then setup to take measurements in either tapping or contact mode. In order to minimise tip wear the force between the tip and the surface was kept to a minimum. Measurements were taken in both air and ultra pure water. In air, silicon tips with a resonant frequency of approximately 300 kHz and a force constant of approximately 40 N/m were used (Tap300Al, Budget Sensors, Sofia, Bulgaria). In liquid and for contact mode measurements, silicon nitride tips with a resonant frequency of

approximately 7 kHz and a force constant of approximately 0.6 N/m were used (DNP-S, Veeco). In liquid, tapping mode was achieved using Z-modulation. To commence a data acquisition run from an array the tip was brought into contact with the first polymer spot, and after completion the tip was raised to a safe height, driven to the next position and lowered into contact with the next spot. Measurements were taken in blocks of 96, after which the alignment and acquisition conditions were checked and the run was then re-commenced. During the block acquisition on 96 samples no user input was required. 5 µm x 5 µm regions of the polymer at 256 lines per image were measured at a frequency of approximately 3 Hz and the root mean square roughness (R_q) was measured across this region. Image processing was conducted using SPIP V3.3.6.0 software (SPIP Metrology, Lyngby, Denmark).

The greatest limitation to high throughput AFM (HT-AFM) studies is the long acquisition times, intrinsic to rastering techniques. The time required to acquire an image for each sample can easily exceed a few minutes depending on the resolution required and the scan speed, which results in a considerable amount of time required to scan hundreds of samples. This can be further compounded if multiple areas on each spot need to be measured to obtain a statistically significant view of the sample surface. As an initial step towards reducing sampling time 24 test samples were imaged at 3 different locations per sample to study the reproducibility across the spot. The average R_q taken from the 3 positions from all 24 samples is plotted in Fig. ESI2 with the standard deviation between the three areas presented as the error bars on each measurement. Significantly, the variance between the measurements taken across a single spot was very small, thus, in this particular case a single measurement from a spot was concluded to be representative for the entire spot, allowing single measurements to be taken for each polymer spot.

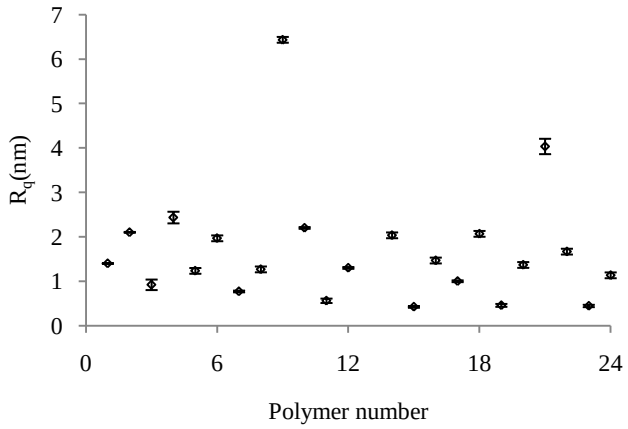

Fig. ESI2. The average values of three R_q measurements taken on 24 test polymers included in the array. The error bars are to 95% confidence. n=3.

ESI3. Comparison of roughness with water contact angle

Previous studies have shown a correlation between water contact angle (WCA) and roughness,[2-4] thus, for each topographical category this relationship was investigated. The static WCA was measured in ambient conditions using the sessile water drop method and plotted against the RMS roughness (R_q) in both liquid and air, shown in Fig. ESI3 for all flat samples. These plots for the other topographical categories are shown in Fig. ESI4. It is clear from Fig. ESI3A that the flat samples have a R_q between 0.5-7 nm, with most falling in the range of 0.5-3 nm when in air, however, the overall R_q is increased when in liquid with all samples within the range of 0.5-20 nm and most samples falling within the range of 0.5-10 nm. This increase in R_q was observed generally across the whole array for all topographies and is likely due to the swelling of the polymers. No trend between R_q and WCA was observed for any of the topographical categories, suggesting that for this particular polymer library the WCA is determined entirely by chemistry. This was confirmed by time-of-flight secondary ion mass spectrometry (ToF-SIMS) analysis coupled with partial least square (PLS) regression that showed a close correlation between the measured WCA and the WCA predicted by the model produced by the regression analysis, with an R^2 value of 0.77 (Fig. ESI5A), but a poor correlation between the measured R_q and the R_q predicted from the PLS model, with an R^2 value of 0.12 (Fig. ESI5B). This demonstrates that the WCA can be predicted by looking only at the chemistry of the sample, thus, the R_q or topography does not significantly contribute to the WCA. Three distinct groups that cluster together as bands were observed in Fig. ESI3, and partially observable in the grouped data shown in Fig. ESI4. The first group is where most polymers are located, and gives a WCA value of between 50-80º when in air. The next group gives heightened WCA from 80-100º, and the final group gives a low WCA between 30-50ºC. These differences can be explained by the chemistry of the monomers involved. The group of highest WCA consists entirely of polymers containing monomer 16, whilst monomers A, B and 1 are present in the low WCA.

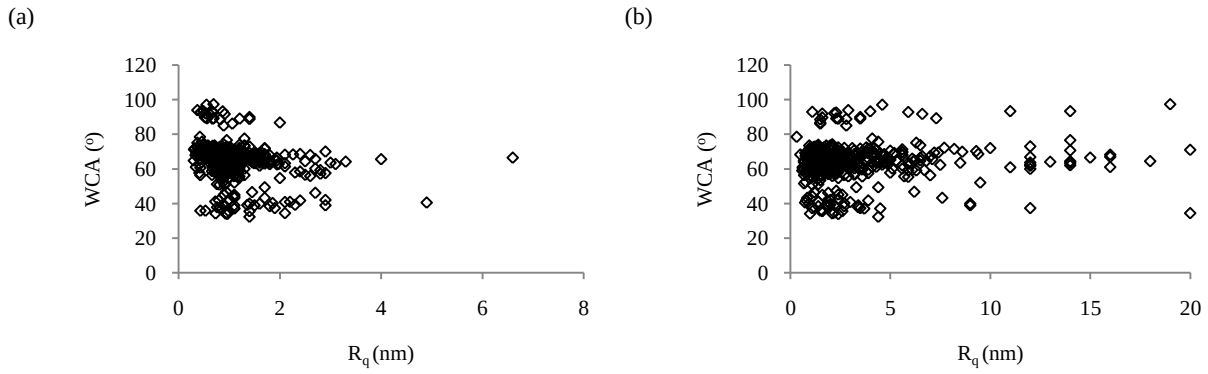

Fig. ESI3. The WCA against the R_q measured in a dry (a) and wet (b) state for all materials in the array.

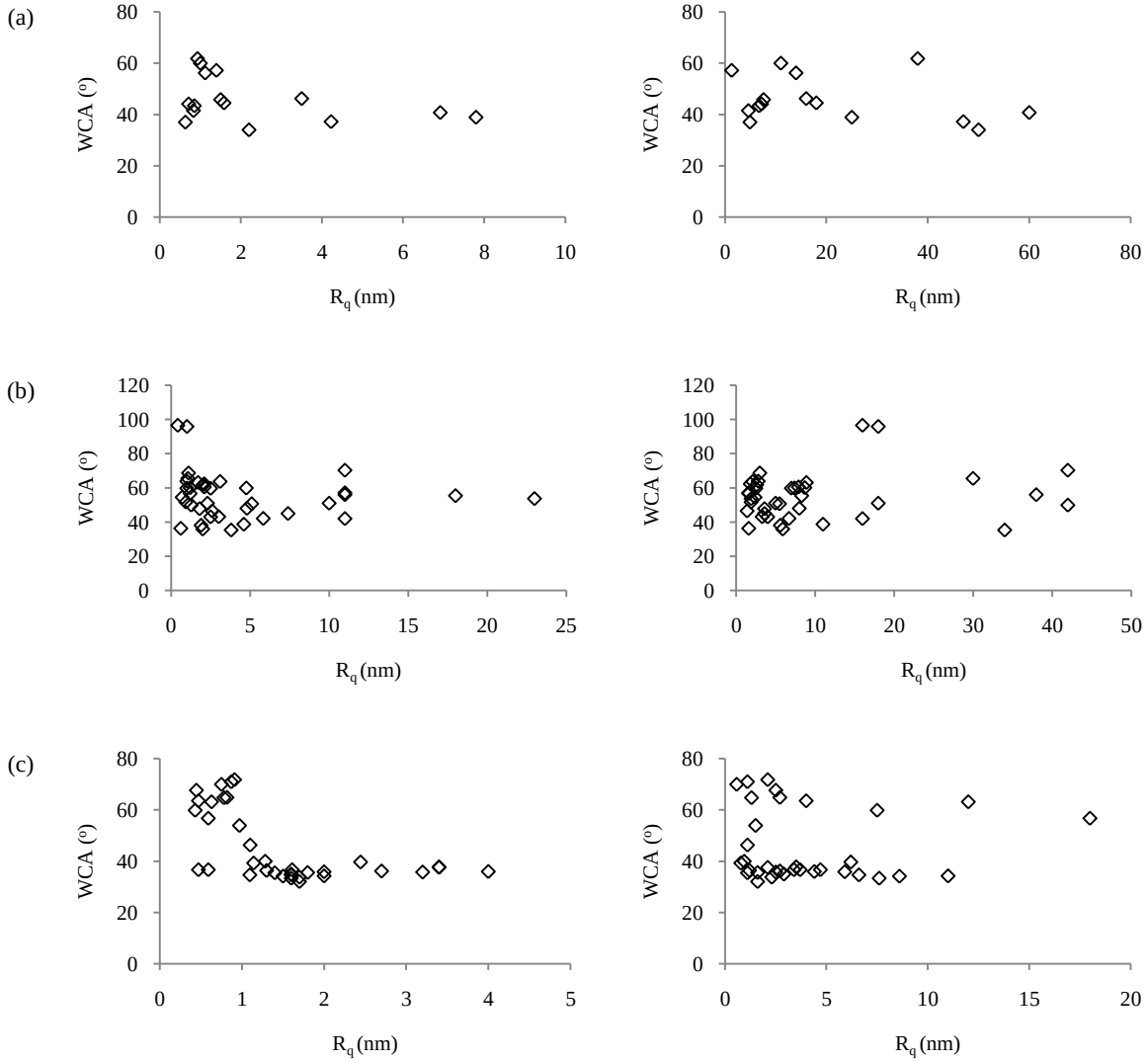

Fig. ESI4. The WCA against the R_q measured in (left) dry state or (right) wet state for materials having (a) pits, (b) nodules or (c) particle nanotopography.

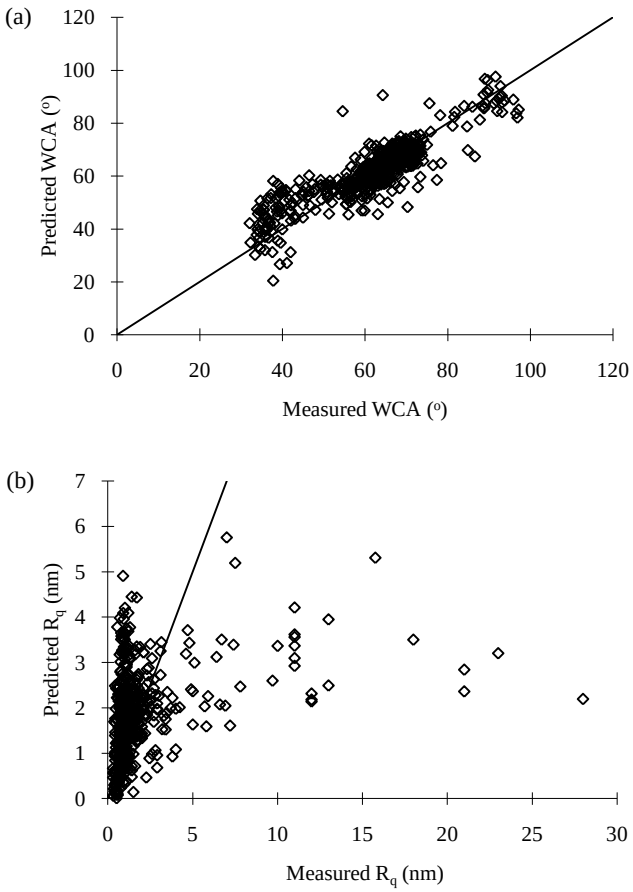

Fig. ESI5. (a) Measured versus predicted WCA and (b) measured versus predicted R_q for the PLS model constructed using the ToF-SIMS spectra from each polymer spot and correlating with the WCA or R_q measured on each spot. The y=x line is drawn as a guide to the eye. R^2=0.77 for a linear fit for (a) and 0.12 for (b).

ESI4. Polymer characterisation

WCA measurements were performed using ultra pure water on a Kruss DSA 100 apparatus fitted with a piezo-doser head. The piezo-doser allowed small ultra pure water (18.2 MΩ.cm) droplets (110 pL) to be deposited onto the polymer spots. Sample positions and data acquisition were automated, with droplet side profiles being recorded (a dual camera system was used, one to record a spot's side profile and the other to record a bird's eye view to ensure that the water droplet was deposited at the centre of each spot) for data analysis. WCA measurement from the image of the drop side profile were performed using iterative fitting of a circle segment function intersecting a straight line representing the suface.[1]

ToF-SIMS analysis was achieved using an ION-TOF ToF-SIMS IV instrument using a monoisotopic Bi_3^+ primary ion source operated at 25 kV in "bunched mode". A 1 pA primary ion beam was rastered and secondary ions were collected from a 100 µm x100 µm area of each polymer spot on the microarray over a 10-second acquisition time. Ion masses were determined using a high resolution Time-of-Flight analyser allowing accurate mass assignment. The typical mass resolution (at m/z 41) was just over 6000. Partial least square (PLS) analysis was carried out using Eigenvector PLS_Toolbox 3.5 for Matlab. The SIMPLS algorithm was used for the PLS analysis. The ToF-SIMS and WCA data were mean-centered before analysis. The SIMS data is a multivariate matrix consisting of ion intensities normalised to the total ion count. The positive and negative ion intensity data was arranged into one concatenated data matrix. 181 positive and 43 negative ions were selected from a group of polymers from the array containing all 22 monomers to form the peak lists. The WCA data is a univariate matrix consisting of WCA number.

ESI5. Topographical categories observed on polymer microarray

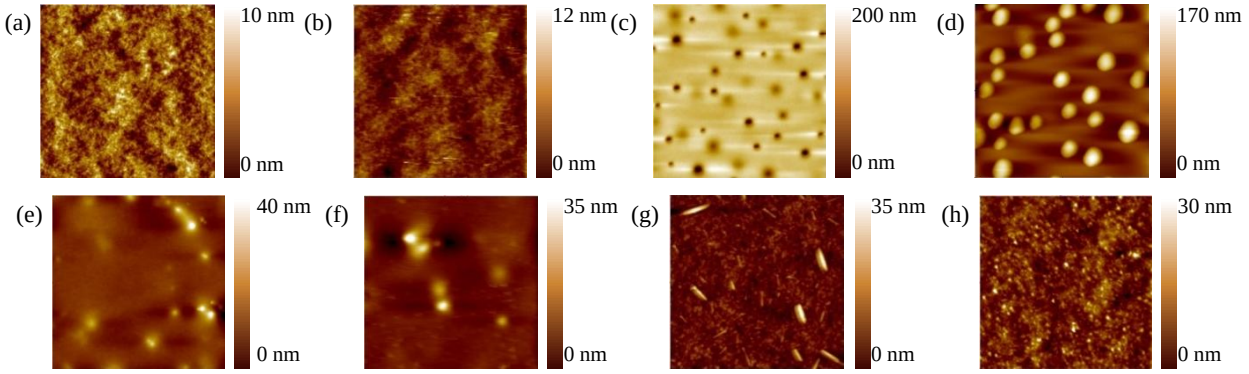

Fig. ESI6. AFM topographical images taken in tapping mode of representative polymer samples fitting four different categories based upon surface features. These categories are (a-b) flat; (c-d) pit (protrusions in water); (e-f) nodules; and (g-h) particles. Each sample is a 5 µm x 5 µm image. The Z-axis, shown alongside each image, is in nm. Images were taken in air (a, c, e, g) or water (b, d, f, h).

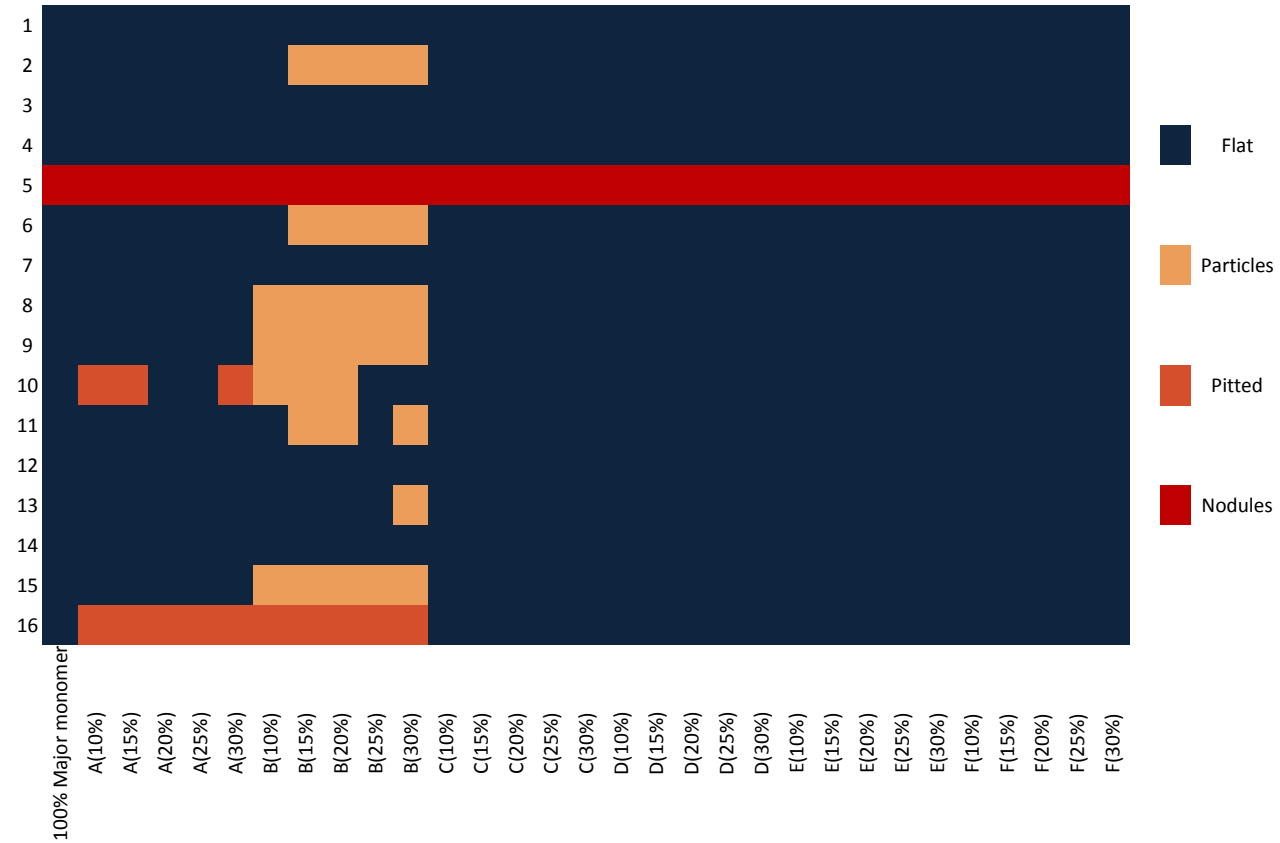

Fig. ESI7. The topographical category for each material in the polymer micro array.

ESI6. AFM images of switchable materials composed of monomers 16 and A or B

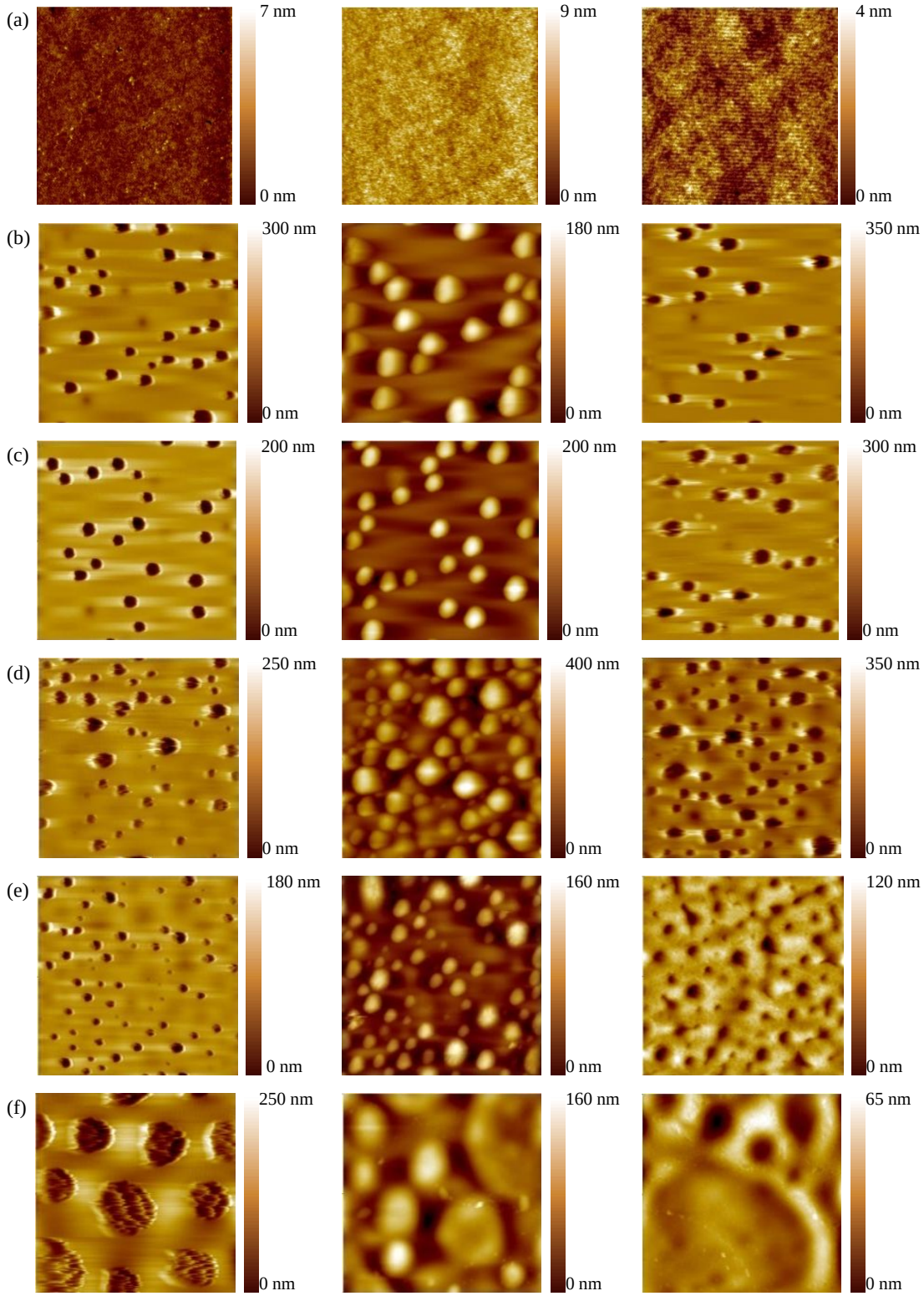

Fig. ESI8. Representative AFM topographical images taken in tapping mode of monomer 16 and A copolymers with varied monomer A content of (a) 0 %; (b) 10 %; (c) 15 %; (d) 20 %; (e) 25 %; (f) 30 %. Samples were initially imaged in air (left image) and then in water (centre image) and subsequently left to dry and imaged again in air (right image). Each image is 5 µm x 5 µm .

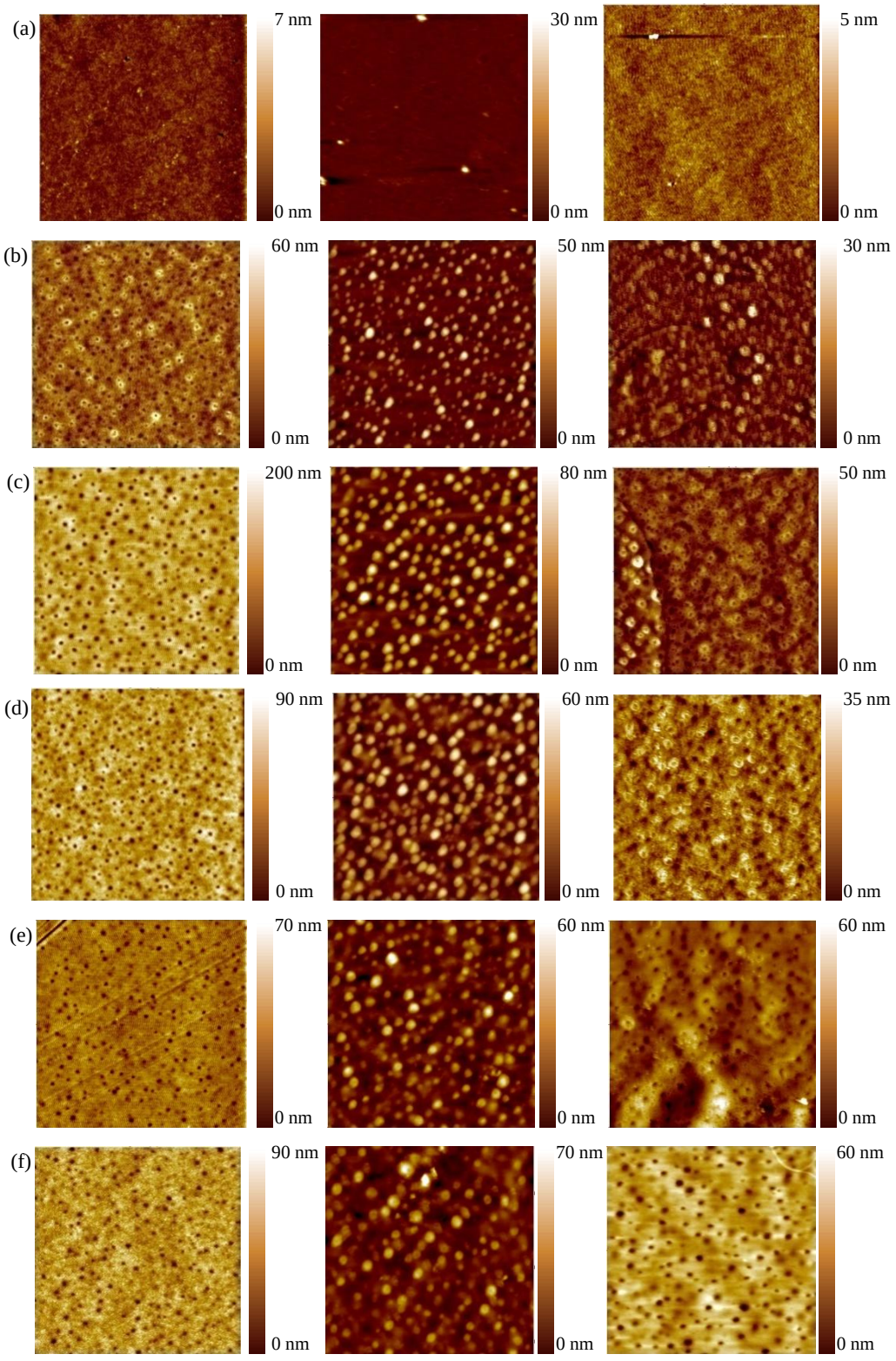

Fig. ESI9. Representative AFM topographical images taken in tapping mode of monomer 16 and B copolymers with varied monomer B content of (a) 0 %; (b) 10 %; (c) 15 %; (d) 20 %; (e) 25 %; (f) 30 %. Samples were initially imaged in air (left image) and then in water (centre image) and subsequently left to dry and imaged again in air (right image). Each image is 5 μm^2.

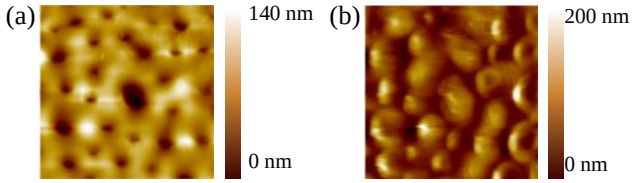

Fig. ESI10. AFM images taken in contact mode of polymer spots composed of 75% (v/v) monomer 16 and 25% (v/v) monomer A in (a) a dry state and (b) a wet state. All images are 5 µm x 5 µm. Representative line-profiles from (c) dried sample of a pit and (d) wet sample of a protrusion.

Table 1. Summary of numerical analysis of pits in copolymers of monomer 16A and 16B. Numbers are shaded to indicate their magnitude, from dark grey to white respectively for high to low values.*

Monomer A content (%)		Feature number per µm^2	Average pit diameter (nm)	Surface coverage of pits (%)	R_q (nm)	WCA (ºC)
Dry	0	0.0	0	0	0.5	96.3
	10	6.2	309	9.6	3.2	46.2
	15	5.2	337	9.3	4.2	37.2
	20	9.8	571	27.8	7.8	38.9
	25	10.8	485	27.4	6.9	40.75
	30	3.6	711	28.6	21.0	44.5
Wet	0	0.0	0	0	2.9	
	10	5.2	594	28.4	34.6	
	15	5.2	471	18.1	23.8	
	20	10.3	493	39.4	34.7	
	25	13.6	390	32.3	25.2	
	30	1.8	1503	63.9	39.3	
Monomer B content (%)						
Dry	0	0.0	0	0	0.5	96.3
	10	44.0	113	8.8	1.1	44.1
	15	48.8	117	10.5	1.2	44.5
	20	60.8	116	12.7	1.4	41.5
	25	41.6	140	12.8	1.1	43.4
	30	30.4	153	11.3	1.4	37
Wet	0	0.0	0	0	2.9	
	10	57.6	169	25.4	6.3	
	15	35.2	243	32.6	13.5	
	20	44.4	223	34.8	11.8	
	25	26.7	267	29.4	8.2	
	30	25.6	309	39.9	6.6	

ESI7. References

1. M. Taylor, A. J. Urquhart, M. Zelzer, M. C. Davies and M. R. Alexander, *Langmuir*, 2007, **23**, 6875-6878.
2. C. T. Hsieh, F. L. Wu and W. Y. Chen, *Materials Chemistry and Physics*, **121**, 14-21.
3. C. J. Lv, C. W. Yang, P. F. Hao, F. He and Q. S. Zheng, *Langmuir*, **26**, 8704-8708.
4. J. Wu, J. Xia, W. Lei and B. P. Wang, *Materials Letters*, **64**, 1251-1253.

* The pits or protrusions were analysed to measure the number of features per µm^2, the diameter, surface coverage, R_q and WCA for copolymers of monomer 16 with monomer A and B in both the dry and wet state. In contrast to other pit dimensions (diameter, surface coverage and R_q), which increased with minor monomer content, the number of pits per unit area increased as monomer content was found to increase from 10% to 25%. A peak in the number of peaks per unit area of 10.8 pits/µm^2 was reached at 25% monomer content and then reduced to 3.6 pits/µm^2 when the minor monomer content was increased to 30%. A similar trend was observed using monomer B as the minor monomer, whereupon a maximum in pit number per unit area of 60.8 pits/µm^2 was observed at a minor monomer content of 20%, which then reduced to 30.4 pits/µm^2 when the minor monomer content was increased to 30%. The same trend was observed when the polymers were exposed to water.

Two effects were observed as a result of increasing the minor monomer content; firstly, the size of the pits increases and secondly the number of pits can increase. At a specific minor monomer content (30%) it became more favourable to form fewer large pits rather than more smaller pits, possibly to allow for the minimisation of the interface between the two phases. The preference for fewer large pits was observed by the significant increase in pit diameter from an average of 485 ± 113 (standard deviation) to 711 ± 182 nm when the minor monomer content was increased from 25% to 30%. Such a change was not observed when monomer B was used as a minor monomer and, furthermore, the pits formed with this monomer were smaller with an average diameter of 128 ± 30 (SD) nm in the dry state as compared with 483 ± 199 (SD) nm for copolymers with monomer A.